INTERNATIONAL JOURNAL FOR NUMERICAL AND ANALYTICAL METHODS IN GEOMECHANICS
Int. J. Numer. Anal. Meth. Geomech. 2005; **29**:941–970
Published online 2 June 2005 in Wiley InterScience (www.interscience.wiley.com). DOI: 10.1002/nag.450

A viscoplastic model including anisotropic damage for the time dependent behaviour of rock

F. Pellet[1,*,†], A. Hajdu[1], F. Deleruyelle[2] and F. Besnus[2]

[1] *Laboratoire Sols Solides Structures (3S), University Joseph Fourier, Grenoble, France*
[2] *Institute for Radiological and Nuclear Safety (IRSN), Clamart, France*

SUMMARY

This paper presents a new constitutive model for the time dependent mechanical behaviour of rock which takes into account both viscoplastic behaviour and evolution of damage with respect to time. This model is built by associating a viscoplastic constitutive law to the damage theory. The main characteristics of this model are the account of a viscoplastic volumetric strain (i.e. contractancy and dilatancy) as well as the anisotropy of damage. The latter is described by a second rank tensor. Using this model, it is possible to predict delayed rupture by determining time to failure, in creep tests for example. The identification of the model parameters is based on experiments such as creep tests, relaxation tests and quasi-static tests. The physical meaning of these parameters is discussed and comparisons with lab tests are presented. The ability of the model to reproduce the delayed failure observed in tertiary creep is demonstrated as well as the sensitivity of the mechanical response to the rate of loading. The model could be used to simulate the evolution of the excavated damage zone around underground openings. Copyright © 2005 John Wiley & Sons, Ltd.

KEY WORDS: viscoplasticity; anisotropic damage; dilatancy; rock; creep test; quasistatic test; time to failure

1. INTRODUCTION

Geomaterials, and rocks in particular, have a complex mechanical behaviour which is often time-dependent. For example, following the application of a stress deviator, non-elastic strains develop as a function of time. If the applied stress deviator is not high enough, these strains will attenuate and stabilize; conversely, if the deviator is high enough, the strain rate starts to accelerate from a certain point, leading to failure of the material.

This behaviour, which has been demonstrated experimentally by several authors for different types of rocks [1–9], can be illustrated by the result of a compression creep test where a primary creep phase is observed during which viscous and strain-hardening phenomena are present,

*Correspondence to: Frédéric Pellet, Laboratoire Sols Solides Structures (3S), University Joseph Fourier, 1301 avenue de la Piscine, 38041 Grenoble, France.
† E-mail: frederic.pellet@hmg.inpg.fr

Received April 2004
Revised January 2005
Accepted March 2005

followed by a secondary creep phase during which only the viscosity phenomenon is active, and a tertiary creep phase corresponding to progressive damage of the material.

In order to model this type of behaviour, viscoplastic models incorporating damage are used. However, most existing constitutive laws do not show the delayed irreversible volumetric strains nor the anisotropy of the damage observed during laboratory tests [10, 11].

The growth of strains and delayed failure phenomena are of vital importance, especially for the design of such structures as underground galleries around which an area of damaged rock develops with time. This zone of damaged rock, often known as the excavated damage zone (EDZ) is of importance for storage structures where the host rock plays a confining role [12, 13].

This paper describes the improvements that have been made to the viscoplastic–damage law proposed by Lemaitre [14]. A parametric study is then presented with a discussion of the physical implications of each parameter. Finally, the model performance is compared with the results of laboratory tests.

2. MODIFICATIONS OF LEMAITRE'S MODEL

2.1. Basic assumptions and thermodynamic framework

Lemaitre's model is a viscoplastic potential model based on the overstress concept proposed by Perzyna [15]. Before describing the changes made to the model, it is worth going over the thermodynamic formalism considered, which is based on the following main hypotheses:

— *Small transformation hypothesis*: The total strain can be considered as the symmetrical part of the displacement gradient operator.
— *Strain partition hypothesis*: The strain is divided into a reversible part (elastic) and an irreversible part (inelastic)

$$\boldsymbol{\varepsilon}^{\mathrm{e}} = \boldsymbol{\varepsilon} - \boldsymbol{\varepsilon}^{\mathrm{vp}} \tag{1}$$

In addition, conditions are assumed to be isothermal, thereby implying zero time-dependent temperature drift, with dissipation being purely mechanical without any thermal dissipation factor. Moreover, the geomechanical stress sign convention is applied; compressive stresses are considered positive.

The model has been drawn up by application of the mechanics of continuous media and the thermodynamics of irreversible processes. This phenomenological approach is based on the local state method which describes the change in the physical phenomena of the medium using a certain number of state variables. Note that for the change process of this set of variables to be permissible from a thermodynamic standpoint, the second principle must be satisfied at each instant in terms of the Clausius–Duhem inequality. Assuming small disturbances, the general Clausius–Duhem inequality is written as follows:

$$\boldsymbol{\sigma} : \dot{\boldsymbol{\varepsilon}} - \rho(\dot{\Psi} + s\dot{T}) - \frac{1}{T}\mathbf{q} \cdot \nabla T \geqslant 0 \tag{2}$$

where $\boldsymbol{\sigma}$ and $\boldsymbol{\varepsilon}$ are, respectively, the stress and strain tensors, ρ the density, Ψ the specific free energy, s the specific entropy, T the absolute temperature and $\mathbf{q}$ the heat flux vector.

If isothermal conditions are considered, this inequality reduces to the following expression:

$$\boldsymbol{\sigma} : \dot{\boldsymbol{\varepsilon}} - \rho\dot{\Psi} \geqslant 0 \tag{3}$$

The state variables define the thermodynamic potential from which the state laws are derived. In the model described here, the Helmholtz specific free energy, Ψ, was used as potential. In order to formulate the viscoplastic model with damage under isothermal conditions, the following state variables are considered:

— total strain $\boldsymbol{\varepsilon}$,
— viscoplastic strain $\boldsymbol{\varepsilon}^{\mathrm{vp}}$,
— cumulative viscoplastic strain, p, associated with the current state of strain hardening of the material, and which is defined by

$$p = \int_0^t \left(\tfrac{2}{3}\dot{\boldsymbol{\varepsilon}}^{\mathrm{vp}}(t) : \dot{\boldsymbol{\varepsilon}}^{\mathrm{vp}}(t)\right)^{1/2} \mathrm{d}t \tag{4}$$

— damage $\mathbf{D}$ (second-order tensor).

The free energy is then expressed as a function of the state variables by

$$\Psi = \Psi(\boldsymbol{\varepsilon}^{\mathrm{e}}, p, \mathbf{D}) \tag{5}$$

and the Clausius–Duhem inequality is expressed in the form

$$\boldsymbol{\sigma} : \dot{\boldsymbol{\varepsilon}} - \rho\dot{\Psi}(\boldsymbol{\varepsilon}^{\mathrm{e}}, p, \mathbf{D}) \geqslant 0 \tag{6a}$$

$$\boldsymbol{\sigma} : \dot{\boldsymbol{\varepsilon}}^{\mathrm{vp}} + \left(\boldsymbol{\sigma} - \rho\frac{\partial\Psi}{\partial\boldsymbol{\varepsilon}^{\mathrm{e}}}\right) : \dot{\boldsymbol{\varepsilon}}^{\mathrm{e}} - \rho\frac{\partial\Psi}{\partial p}\dot{p} - \rho\frac{\partial\Psi}{\partial\mathbf{D}} : \dot{\mathbf{D}} \geqslant 0 \tag{6b}$$

The variables of thermodynamic forces associated, respectively, with elastic strain, with the strain-hardening variable and with the damage, can then be deduced

$$\boldsymbol{\sigma} = \rho\frac{\partial\Psi}{\partial\boldsymbol{\varepsilon}^{\mathrm{e}}} \tag{7}$$

$$R = \rho\frac{\partial\Psi}{\partial p} \tag{8}$$

$$\mathbf{Y} = \rho\frac{\partial\Psi}{\partial\mathbf{D}} \tag{9}$$

Given that thermal dissipation is zero, the dissipation power, Φ, is purely intrinsic (i.e. of mechanical origin) and is written as follows:

$$\Phi = \boldsymbol{\sigma} : \dot{\boldsymbol{\varepsilon}}^{\mathrm{vp}} - R\dot{p} - \mathbf{Y} : \dot{\mathbf{D}} \geqslant 0 \tag{10}$$

The change laws of the flux variables ($\dot{\boldsymbol{\varepsilon}}^{\mathrm{vp}}, \dot{p}$ and $\dot{\mathbf{D}}$) are determined from a dissipation potential φ

$$\boldsymbol{\sigma} = \frac{\partial\varphi}{\partial\dot{\boldsymbol{\varepsilon}}^{\mathrm{vp}}} \tag{11}$$

$$R = -\frac{\partial \varphi}{\partial \dot{p}} \tag{12}$$

$$\mathbf{Y} = -\frac{\partial \varphi}{\partial \dot{\mathbf{D}}} \tag{13}$$

However, as a general rule, it is more practical to express the change in force variables as a function of flux variables. A Legendre–Fenchel transform is used to define a dual potential (φ^*) where the evolution laws are written as follows:

$$\dot{\boldsymbol{\varepsilon}}^{\mathrm{vp}} = \frac{\partial \varphi *}{\partial \boldsymbol{\sigma}} \tag{14}$$

$$\dot{p} = -\frac{\partial \varphi^*}{\partial R} \tag{15}$$

$$\dot{\mathbf{D}} = -\frac{\partial \varphi^*}{\partial \mathbf{Y}} \tag{16}$$

The intrinsic dissipation power as a function of the dual dissipation potential is ultimately obtained by

$$\Phi = \boldsymbol{\sigma} : \frac{\partial \varphi *}{\partial \boldsymbol{\sigma}} + R\frac{\partial \varphi^*}{\partial R} + \mathbf{Y} : \frac{\partial \varphi^*}{\partial \mathbf{Y}} \geqslant 0 \tag{17}$$

In order for the inequality to be satisfied, the following conditions are imposed on the dissipation potential:

— φ^* must be a convex function of the variables $\boldsymbol{\sigma}$, R and $\mathbf{Y}$,
— φ^* must always be positive,
— φ^* must contain the origin, i.e. it must cancel out for $\sigma_{ij} = p = Y_{ij} = 0$.

The second principle of thermodynamics is therefore satisfied because the intrinsic dissipation is non-negative

$$\Phi \geqslant 0 \tag{18}$$

For the model presented below, and in order to simplify the formulation, the dissipation potential was broken down into two parts

$$\varphi = \Omega^{\mathrm{vp}}(\boldsymbol{\varepsilon}^{\mathrm{vp}}, p) + \Omega^{\mathrm{D}}(\mathbf{D}) \tag{19}$$

or in terms of the dual potential

$$\varphi^* = \Omega^{\mathrm{vp}}(\boldsymbol{\sigma}, R) + \Omega^{\mathrm{D}}(\mathbf{Y}) \tag{20}$$

The first term on the right-hand side of the equation (Ω^{vp}) corresponds to the strain and strain-hardening processes, whereas the second term (Ω^{D}) corresponds to the damaging process. This specific distinction is standard practice and is based on the assumption that the two dissipation processes are independent and governed by two distinct additive potentials. If the two potentials separately satisfy the convexity and non-negativity criteria, so does their sum. It therefore suffices to analyse them separately.

2.2. *Viscoplastic law with irreversible volumetric strain*

First, only viscous phenomena are modelled, with the delayed damage being ignored, but taking into account the volumetric strain.

The classical approach in elasto-viscoplasticity consists in defining a load surface in the stress space inside which the stress states cause entirely reversible strains. The framework of viscoplastic process thermodynamics, briefly summarized above, is based on the concept of equipotential surfaces. The viscoplastic law is entirely defined by the dissipation potential, thus enabling the rate of viscoplastic strain to be calculated directly by applying the normality rule.

In its original version, Lemaitre's law makes use of the von Mises load surface which is not suited to geomaterials because it does not provide an inelastic volumetric strain. Using the procedure proposed by Lemaitre and Chaboche [14], but by introducing a load surface depending not only on the second deviator invariant but also on the first stress invariant, and by assuming isotropic strain hardening, the following expression is obtained for dissipation potential:

$$\Omega^{\mathrm{vp}} = \frac{K}{N+1}\left\langle \frac{f(J_2;I_1)}{K} \right\rangle^{N+1} p^{-N/M} \tag{21}$$

where Ω^{vp} is the dissipation potential, M, N and K are viscoplastic coefficients. The state of strain hardening is expressed by the variable p.

Note the multiplicative separation of the variables; the first part represents the perfect viscoplastic potential multiplied by the strain hardening function.

Consequently, the power function form of the dissipation potential proposed by Lemaitre has been retained, replacing the von Mises criterion by a Drucker–Prager type criterion [16]. The expression of the load surface $f(J_2;I_1)$ indicates the equipotential surface function. This function is written as follows:

$$f(J_2;I_1) = \sigma_{\mathrm{eq}} + \alpha\sigma_{\mathrm{m}} - k \tag{22}$$

with

$$\sigma_{\mathrm{eq}} = \sqrt{\tfrac{3}{2}\mathbf{S}:\mathbf{S}} \tag{23}$$

$$\mathbf{S} = \boldsymbol{\sigma} - \tfrac{1}{3}\mathrm{tr}(\boldsymbol{\sigma})\cdot\mathbf{I} \tag{24}$$

$$\sigma_{\mathrm{m}} = \tfrac{1}{3}\mathrm{tr}(\boldsymbol{\sigma}) \tag{25}$$

$$I_1 = \mathrm{tr}(\boldsymbol{\sigma}) = 3\sigma_{\mathrm{m}} \tag{26}$$

where $\boldsymbol{\sigma}$, $\mathbf{I}$ and $\mathbf{S}$ are, respectively, the stress tensor, the identity tensor and the stress deviator.

The parameter α in Equation (22), is used to characterize the delayed volumetric strain. It is linked to the dilatancy angle, ψ, by the relation

$$\alpha = \tan(\psi) \tag{27}$$

The coefficient k in (22) enables the viscoplasticity threshold to be defined. However, the viscoplasticity threshold often appears to be very low, which is mathematically equivalent to

assuming that $k = 0$. In what follows, $k = 0$ is assumed, and the function $f(J_2; I_1)$ is written as

$$f(J_2; I_1) = \sigma_{\text{eq}} + \alpha\sigma_{\text{m}} \tag{28}$$

It is also worth noting that the Drucker–Prager criterion has well known drawbacks. In particular, it gives the same plasticity threshold under compression as under tensile stress, a fact that is not in agreement with the observations made on most geomaterials. Moreover, not all cone opening angles are physically permissible [17].

However, in viscoplasticity the consistency rule no longer applies [18]. The state of stresses must be located outside the load surface in order for viscoplastic flow to occur. The strain rate increases with distance from this 'overstress' with respect to the load surface where the flow is infinitely slow. We therefore have a family of surfaces and, in each point on a given surface, the strain rate modulus (or, in other words, the dissipation) is identical. The viscoplastic dissipation potential can therefore be written as follows:

$$\Omega^{\text{vp}} = \frac{K}{N+1}\left\langle \frac{\sigma_{\text{eq}} + \alpha\sigma_{\text{m}}}{K} \right\rangle^{N+1} p^{-N/M} \tag{29}$$

The viscoplastic strain rate is deduced from the dissipation potential simply by application of the normality rule, i.e.

$$\dot{\boldsymbol{\varepsilon}}^{\text{vp}} = \frac{\partial \Omega^{\text{vp}}}{\partial \boldsymbol{\sigma}} \tag{30a}$$

$$\dot{\boldsymbol{\varepsilon}}^{\text{vp}} = \frac{\partial \Omega^{\text{vp}}}{\partial \sigma_{\text{eq}}}\frac{\partial \sigma_{\text{eq}}}{\partial \boldsymbol{\sigma}} + \frac{\partial \Omega^{\text{vp}}}{\partial \sigma_{\text{m}}}\frac{\partial \sigma_{\text{m}}}{\partial \boldsymbol{\sigma}} \tag{30b}$$

$$\dot{\boldsymbol{\varepsilon}}^{\text{vp}} = \left\langle \frac{\sigma_{\text{eq}} + \alpha\sigma_{\text{m}}}{K p^{1/M}} \right\rangle^{N} \left(\frac{3}{2}\frac{\mathbf{S}}{\sigma_{\text{eq}}} + \frac{\alpha \mathbf{I}}{3} \right) \tag{30c}$$

Considering isotropic strain hardening of the material and assuming that there is no recovery process, the value of the variable is still increasing. The cumulative viscoplastic strain can therefore be used as an indicator of the state of strain hardening of the material. This is calculated by

$$\dot{p} = \sqrt{\tfrac{2}{3}\dot{\boldsymbol{\varepsilon}}^{\text{vp}} : \dot{\boldsymbol{\varepsilon}}^{\text{vp}}} \tag{31}$$

In this case, we obtain

$$\dot{p} = \sqrt{\frac{2}{9}\alpha^2 + 1}\left\langle \frac{\sigma_{\text{eq}} + \alpha\sigma_{\text{m}}}{K p^{1/M}} \right\rangle^{N} \tag{32}$$

Because $\mathbf{I} : \mathbf{I} = 3$, $\mathbf{I} : \mathbf{S} = 0$ and $\mathbf{S} : \mathbf{S} = \frac{2}{3}\boldsymbol{\sigma}_{\text{eq}}^2$, the viscoplastic strain rate to be expressed in the following form:

$$\dot{\boldsymbol{\varepsilon}}^{\text{vp}} = \dot{p}\left(\frac{2}{9}\alpha^2 + 1 \right)^{-1/2} \left(\frac{3}{2}\frac{\mathbf{S}}{\sigma_{\text{eq}}} + \frac{\alpha \mathbf{I}}{3} \right) \tag{33}$$

Lemaitre's model has therefore been enriched by an additional parameter α that will be called the dilatancy parameter. As far as hydrostatic loading is concerned, it should be noted that, for a contracting material, ($\alpha > 0$), no viscoplastic flow occurs under tensile stress and, similarly,

a dilatant material ($\alpha<0$) does not flow under compressive stress, a fact that is physically acceptable.

The influence of the dilatancy parameter α on the delayed bulk behaviour for an elastically compressible material ($v<0.5$) subjected to constant loading can be illustrated. Following an instantaneous elastic contractancy, viscoplastic volumetric strains appear due to creep. For positive values of α the delayed behaviour is contractive whereas the negative values generate dilatancy. By setting $\alpha = 0$ the viscoplastic volumetric strains disappear, and the model reverts to Lemaitre's original form.

Note that from a thermomechanical standpoint, the expression [19] is not a standard law *stricto sensu* because the parameter, p, takes part in the dissipation potential. This is a characteristic of multiplicative strain hardening/viscosity laws which require the introduction of a further condition, in addition to the generalized normality law, in order to guarantee the Clausius–Duhem condition. One solution consists in assuming that the free energy is independent of p, in which case R (Equation (12)) cancels out. It can then be said that Ω^{vp} is a convex function on condition that the parameter N is positive. For $\boldsymbol{\sigma} = \mathbf{0}$ ($R = 0$), $\Omega^{vp} = 0$ is obtained and the potential therefore effectively contains the origin.

The mechanical power dissipated by the viscoplastic process is then expressed by

$$\Phi^{vp} = \boldsymbol{\sigma} : \frac{\partial \Omega^{vp}}{\partial \boldsymbol{\sigma}} - R\frac{\partial \Omega^{vp}}{\partial R} \tag{34a}$$

$$\Phi^{vp} = \boldsymbol{\sigma} : \dot{\boldsymbol{\varepsilon}}^{vp} - R\dot{p} \tag{34b}$$

with $R = 0$, the dissipation is reduced to

$$\Phi^{vp} = \boldsymbol{\sigma} : \dot{\boldsymbol{\varepsilon}}^{vp} \tag{34c}$$

2.3. Law of induced anisotropic damage

In this section an appropriate description is proposed for delayed damage mechanisms by introducing a tensorial damage variable and by defining a time-dependent law for this variable.

Experimental observations have highlighted anisotropic damage in rocks [7]. Under a low average stress, mechanically induced microcracks are generated in extension mode (mode I), and continue to grow in the main stress direction, thereby inducing an anisotropy in the mechanical properties [6]. This induced anisotropy is therefore the result of a change in rock damage which expresses the progressive deterioration of the cohesion of the material. This causes general dilatation of the rock and subsequently leads to delayed failure.

Lemaitre's viscoplastic law is classically coupled with isotropic damage described by a scalar damage variable, D, which cannot express the anisotropy of damage. Several authors [20, 21] have shown that the geometrical properties of a given damage state can be correctly described by a second-order symmetrical tensor. The main limitation of this approach is that, in the most general case, the damage described has an orthotropic symmetry where the orthotropic axes are identified with the main directions of the damage tensor. However, this limitation is acceptable when modelling most geomaterials, and a second-order symmetrical tensor, $\mathbf{D}$, can be chosen to express the damage anisotropy.

The description of material damage is based on the concept of effective stress [22–24]. Various proposals can be found in the literature regarding the formulation of a symmetrical effective

stress tensor linked to a second-order damage tensor. In the model described here, the effective stress, $\tilde{\boldsymbol{\sigma}}$, is defined as follows:

$$\tilde{\boldsymbol{\sigma}} = (\mathbf{I} - \mathbf{D})^{-1/2} \cdot \boldsymbol{\sigma} \cdot (\mathbf{I} - \mathbf{D})^{-1/2} \tag{35}$$

This expression, derived from the energy equivalence principle, was proposed by Cordebois and Sidoroff [25]. Contrary to a formulation based on the strain equivalence principle, it has the advantage of automatically ensuring the symmetry of the effective stress tensor. Assuming that the viscoplastic and damage processes dissipate independently, the dissipation potential can be written as follows:

$$\Omega^{\mathrm{D}} = \tfrac{1}{2}\mathbf{Y} : \overset{=4=}{\mathbf{S}} : \mathbf{Y} \tag{36}$$

where $\mathbf{Y}$ is the thermodynamic force associated with the damage (second-order tensor) and $\mathbf{S}^{=4=}$ a fourth-order tensor, referred to the structure tensor.

The damage evolution law is then written as

$$\dot{\mathbf{D}} = \frac{\partial \Omega^{\mathrm{D}}}{\partial \mathbf{Y}} = \overset{=4=}{\mathbf{S}} : \mathbf{Y} \tag{37}$$

The damage effects are represented by the effective stress, $\tilde{\boldsymbol{\sigma}}$, which is substituted in the constitutive equations in place of the stress actually applied and the damage variable. Thus

$$\dot{\boldsymbol{\varepsilon}}(\boldsymbol{\sigma}, \mathbf{D}, \ldots) = \dot{\boldsymbol{\varepsilon}}(\tilde{\boldsymbol{\sigma}}, \ldots) \tag{38}$$

The time-dependent change in damage also depends on the state of applied stress and the present state of damage of the material. It is possible to represent them by a fictitious driving stress, $\hat{\boldsymbol{\sigma}}$, which appears in the damage change equation in place of the stress actually applied and the damage variable

$$\dot{\mathbf{D}}(\boldsymbol{\sigma}, \mathbf{D}, \ldots) = \dot{\mathbf{D}}(\hat{\boldsymbol{\sigma}}, \ldots) \tag{39}$$

This approach was proposed by Qi and Bertram [26]. For the driving stress, the following form has been considered:

$$\hat{\boldsymbol{\sigma}} = [(\mathbf{I} - \mathbf{D})/\det(\mathbf{I} - \mathbf{D})]^{q/2} \cdot \boldsymbol{\sigma} \cdot [(\mathbf{I} - \mathbf{D})/\det(\mathbf{I} - \mathbf{D})]^{q/2} \tag{40}$$

In this expression, q is a parameter of the material enabling the damage effect on the strain rate to be distinguished from its own evolution (Figure 10(a)). This distinction is necessary because experimental observations show that the influence of damage is greater on the damage growth rate than on overall mechanical behaviour. Using $\hat{\boldsymbol{\sigma}}$ the thermodynamic force associated with the damage can be defined as

$$\mathbf{Y} = \left\langle \frac{t\hat{\boldsymbol{\sigma}}}{A} \right\rangle^{r} = \sum_{i=1}^{3} \left\langle \frac{t\hat{\sigma}_i}{A} \right\rangle^{r} \vec{\hat{\mathbf{s}}}_i \otimes \vec{\hat{\mathbf{s}}}_i \tag{41}$$

where A and r are material parameters, $\hat{\sigma}_i$ and $\vec{\hat{\mathbf{s}}}_i$ the eigenvalues and the eigenvectors of $\hat{\boldsymbol{\sigma}}$, respectively, t indicates the state of triaxiality of the stresses and is expressed by

$$t = \frac{\sigma_{\mathrm{eq}}}{3\sigma_{\mathrm{m}}} \tag{42}$$

Note that the positivity imposed on $\mathbf{Y}$ does not exclude damage change by tensile stresses (negative stresses) because of the presence of the triaxiality term in the expression. The only non-permissible stress state is the special case where $\sigma_m = 0$ but $\sigma_{eq} \neq 0$.

The structure tensor links the damage driving forces to its structural change by taking the following form:

$$\overset{=4=}{\mathbf{S}} = (\beta - 1)\overset{=4=}{\mathbf{I}} + \mathbf{I} \otimes \mathbf{I} \tag{43}$$

where $\mathbf{I}^{=4=}$ is the fourth-order unit tensor and β the anisotropy parameter of the model.

This parameter β expresses the degree of anisotropy of damage change. $\beta = 1$ corresponds to isotropic change whereas $\beta = 0$ models an anisotropic change where the damage extends only in the direction perpendicular to the driving stress. Obviously, β can take any real intermediate value. Figure 1 shows the value of the parameter β for the two extreme configurations. The damage evolution law is finally expressed by

$$\dot{\mathbf{D}} = \overset{=4=}{\mathbf{S}} : \mathbf{Y} = ((\beta - 1)\overset{=4=}{\mathbf{I}} + \mathbf{I} \otimes \mathbf{I}) : \sum_{i=1}^{3} \left\langle \frac{t\hat{\sigma}_i}{A} \right\rangle^r \vec{\hat{\mathbf{s}}}_i \otimes \vec{\hat{\mathbf{s}}}_i \tag{44}$$

It can be shown that the form of the structure tensor implies that the eigenvectors of the damage rate tensor have the same orientation as those of the driving stress tensor. The material fails when one eigenvalue of $\mathbf{D}$ reaches a critical value $D_{crit.} = 1$.

For uniaxial stress application, with isotropic change ($\beta = 1$) and by letting $qr \equiv k$, we obtain the classic expression proposed by Kachanov [27] and Rabotnov [28], for describing damage growth in tertiary creep.

It is also worth noting that the unilateral effects relating to the closure and thus deactivation of microcracks have not been taken into account. In the absence of cyclic stress applications, it is useful to integrate the deactivation conditions in the model. Finally, the damage as defined in Equation (44) is always increasing or constant; in other words, the 'healing' of the material is not incorporated in the model. The damage dissipation potential

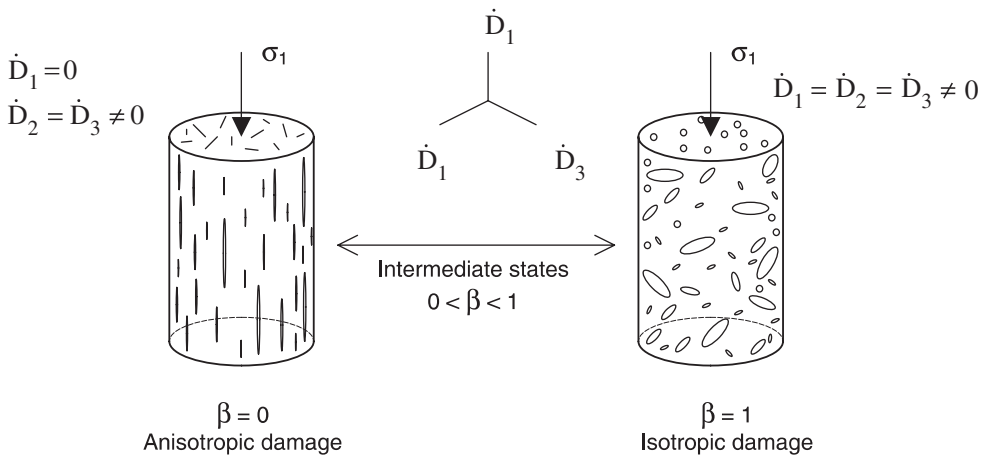

Figure 1. Illustration of the significance of the parameter, β, for an uniaxial compressive test.

is therefore defined by

$$\Omega^{\mathrm{D}} = \tfrac{1}{2}\mathbf{Y} : \overset{=4=}{\mathbf{S}} : \mathbf{Y} \tag{45}$$

Ω^{D} is a convex function (quadratic) in $\mathbf{Y}$. For $\mathbf{Y} = 0$ it cancels out. In addition, the intrinsic damage dissipation is always positive or zero. It is written by

$$\Phi^{\mathrm{D}} = \mathbf{Y} : \frac{\partial \Omega^{\mathrm{D}}}{\partial \mathbf{Y}} \tag{46}$$

The fourth-order tensor $\mathbf{S}^{=4=}$ (structure tensor) is defined as being symmetrical and positive in the main reference frame of the driving forces with $0 \leqslant \beta \leqslant 1$. Given that the Macaulay brackets in $\mathbf{Y}$ guarantee the positivity of the driving tensor, the thermodynamic restrictions are therefore satisfied.

2.4. Coupling of viscoplasticity and damage

It is now possible to couple the viscoplastic law with irreversible volumetric strain, and the anisotropic damage law. The advantage of coupling lies in the fact that the stress and strain response of the material depends not only on viscous mechanisms but also, simultaneously, on the damage. Coupled calculations provide a means of obtaining the stress, strain and damage states at any moment.

In order to describe the behaviour of a viscoplastic material capable of being work-hardened and damaged, the equivalence principle is applied by replacing the stress $\boldsymbol{\sigma}$ by the effective stress $\tilde{\boldsymbol{\sigma}}$ defined by Equation (35).

This modification concerns all strains. The partition hypothesis divides the total strain into an elastic and an inelastic part. Formulation of consistency requires replacing the stress by the effective stress in the stress vs elastic and viscoplastic strain relations. The isotropic elastic behaviour is therefore described by Hooke's coupled law

$$\dot{\boldsymbol{\varepsilon}}^{\mathrm{e}} = \frac{1+v}{E}\dot{\tilde{\boldsymbol{\sigma}}} - \frac{v}{E}\,\mathrm{tr}(\dot{\tilde{\boldsymbol{\sigma}}}) \cdot \mathbf{I} \tag{47}$$

In the viscoplastic formalism, the only term affected by this change is the dissipation potential, the other variables of the viscoplastic model remaining unchanged. The potential is then written as

$$\Omega^{\mathrm{vp}} = \frac{K}{N+1}\left\langle \frac{f(\tilde{J}_2; \tilde{I}_1)}{K} \right\rangle^{N+1} p^{-N/M} \tag{48}$$

It can be seen that the potential keeps its multiplicative form, and that the viscoplastic coefficients (M, N and K) remain the same. Only the equipotential surface function is subject to modifications, this being a natural consequence of applying the equivalence principle. The effective stress replaces the stress value in the calculation of the invariants and thus defines a new equipotential surface as a function of the damage state of stresses. The viscous and damage states are then coupled. This new equipotential surface is

$$f(\tilde{J}_2; \tilde{I}_1) = \tilde{\sigma}_{\mathrm{eq}} + \alpha \tilde{\sigma}_{\mathrm{m}} \tag{49}$$

where $\tilde{\sigma}_{eq}$ is the equivalent effective stress

$$\tilde{\sigma}_{eq} = \sqrt{\tfrac{3}{2}\tilde{\mathbf{S}} : \tilde{\mathbf{S}}} \tag{50}$$

with $\tilde{\mathbf{S}}$ the effective stress deviator

$$\tilde{\mathbf{S}} = \tilde{\boldsymbol{\sigma}} - \tfrac{1}{3}\mathrm{tr}\tilde{\boldsymbol{\sigma}} \cdot \mathbf{I} \tag{51}$$

and $\tilde{\sigma}_m$ the mean effective stress

$$\tilde{\sigma}_m = \tfrac{1}{3}\mathrm{tr}\tilde{\boldsymbol{\sigma}} \tag{52}$$

The parameter α, defined previously, expresses the dilatancy. This parameter is not influenced by the damage, i.e. the effects of the damage are superimposed on the viscosity effects. This separation enables more complex volumetric behaviour to be simulated (for example, contractive in a first stage and then dilatant).

The effective stress is calculated, as a function of the nominal stress and the damage variable, the evolution law of which was developed in Equations (37)–(44).

The viscoplastic strain rate is deduced, as seen in Equations (30a)–(30c), by application of the normality rule to the dissipation potential. Obviously, for the coupled model, the strain rate is obtained from the viscoplastic dissipation potential, modified according to Equation (48)

$$\dot{\boldsymbol{\varepsilon}}^{vp} = \frac{\partial \Omega^{vp}}{\partial \boldsymbol{\sigma}} \tag{53a}$$

$$\dot{\boldsymbol{\varepsilon}}^{vp} = \frac{\partial \Omega^{vp}}{\partial \tilde{\sigma}_{eq}} \frac{\partial \tilde{\sigma}_{eq}}{\partial \boldsymbol{\sigma}} + \frac{\partial \Omega^{vp}}{\partial \tilde{\sigma}_m} \frac{\partial \tilde{\sigma}_m}{\partial \boldsymbol{\sigma}} \tag{53b}$$

$$\dot{\boldsymbol{\varepsilon}}^{vp} = \left\langle \frac{\tilde{\sigma}_{eq} + \alpha \tilde{\sigma}_m}{K p^{1/M}} \right\rangle^N (\mathbf{I} - \mathbf{D})^{-1/2} \cdot \left(\frac{3}{2} \frac{\tilde{\mathbf{S}}}{\tilde{\sigma}_{eq}} + \frac{\alpha \mathbf{I}}{3} \right) \cdot (\mathbf{I} - \mathbf{D})^{-1/2} \tag{53c}$$

$$\dot{\boldsymbol{\varepsilon}}^{vp} = \left\langle \frac{\tilde{\sigma}_{eq} + \alpha \tilde{\sigma}_m}{K p^{1/M}} \right\rangle^N \left(\frac{3}{2} \frac{\tilde{\tilde{\mathbf{S}}}}{\tilde{\sigma}_{eq}} + \frac{\alpha (\mathbf{I} - \mathbf{D})^{-1}}{3} \right) \tag{53d}$$

with the notation

$$\tilde{\tilde{\mathbf{S}}} \equiv (\mathbf{I} - \mathbf{D})^{-1/2} \cdot \tilde{\mathbf{S}} \cdot (\mathbf{I} - \mathbf{D})^{-1/2} \tag{54}$$

The state of material strain hardening, still characterized by the cumulative viscoplastic strain, is calculated from

$$\dot{p} = \sqrt{\frac{2}{3}} \left\langle \frac{\tilde{\sigma}_{eq} + \alpha \tilde{\sigma}_m}{K p^{1/M}} \right\rangle^N \left\| \left(\frac{3}{2} \frac{\tilde{\tilde{\mathbf{S}}}}{\tilde{\sigma}_{eq}} + \frac{\alpha (\mathbf{I} - \mathbf{D})^{-1}}{3} \right) \right\| \tag{55}$$

where the sign || || designates the Euclidian norm. This allows the constitutive law to be written in the following final form:

$$\dot{\boldsymbol{\varepsilon}}^{\mathrm{vp}} = \sqrt{\frac{3}{2}}\dot{p}\frac{\left(\frac{3}{2}\frac{\tilde{\tilde{\mathbf{S}}}}{\tilde{\sigma}_{\mathrm{eq}}} + \frac{\alpha(\mathbf{I}-\mathbf{D})^{-1}}{3}\right)}{\left\|\left(\frac{3}{2}\frac{\tilde{\tilde{\mathbf{S}}}}{\tilde{\sigma}_{\mathrm{eq}}} + \frac{\alpha(\mathbf{I}-\mathbf{D})^{-1}}{3}\right)\right\|} \tag{56}$$

3. STUDY OF THE PARAMETERS INFLUENCE BASED ON TESTS RESULTS

3.1. Types of tests and definition of parameters

This section presents a parametric study and the modelling of tests results. The influence and the physical implications of each of these parameters is discussed. To determine the mechanical properties of a damageable viscoplastic material, simple tests such as monotonous loading tests, creep tests and relaxation tests, have to be performed.

To highlight the role of each parameter, each type of test was simulated by considering a set of parameters representative of a soft rock. These simulations were carried out for a uniaxial compressive loading. The new viscoplastic model incorporating damage, previously presented in tensorial form for the general three-dimensional case, is given in Appendix A for uniaxial loading. The meaning and denomination of the parameters as well as the values considered are given below

N is the viscosity exponent,	$2 < N < 100$
M is the strain-hardening parameter,	$2 < M < 50$
K is the viscoplastic stiffness coefficient,	$50 < K < 100\,000$ MPa s
r is the damage exponent,	$1 < r < 20$
q is the damage progression parameter,	$0 < q < 1$
A is the tenacity coefficient	$10 < A < 1000$ MPa s

3.2. Viscoplastic and damage parameters

Consider the coupled viscoplastic model with damage. In a first stage, the value of the viscoplastic dilatancy-contractancy parameter, α, is kept equal to 0 (no viscoplastic volumetric strain) and the value of the damage anisotropy parameter, β, is equal to 1 (isotropic damage). A detailed discussion, presented in the section, is devoted to a study of the influence of these two variables.

3.2.1. Viscosity exponent N. The sensitivity of the model to the viscosity exponent, N, is shown on Figures 2 and 3. For each type of test (monotonous strain-controlled loading, creep, relaxation) two values of N were studied. Two loading strain rates ($\dot{\varepsilon} = \dot{\varepsilon}_0$ and $\dot{\varepsilon} = 100\dot{\varepsilon}_0$) for the monotonous loading test and three levels of initial relaxation stress ($0.3R_{\mathrm{c}}$, $0.6R_{\mathrm{c}}$ and $0.9R_{\mathrm{c}}$ where R_{c} is the uniaxial compressive strength) were simulated (Figure 4).

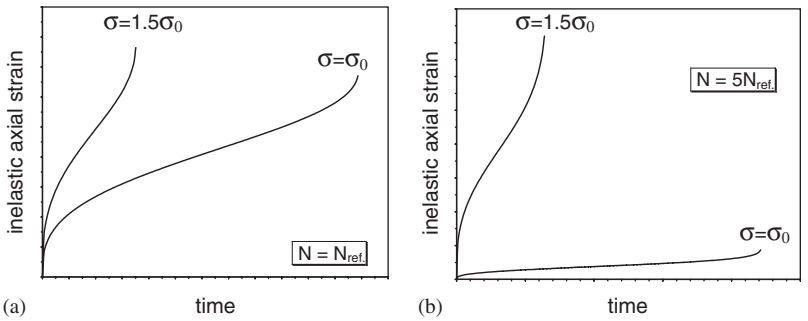

Figure 2. Inelastic axial strain versus time for different stresses (creep tests): (a) low value of viscosity exponent ($N = N_{\text{ref}}$); and (b) high value of viscosity exponent ($N = 5N_{\text{ref}}$).

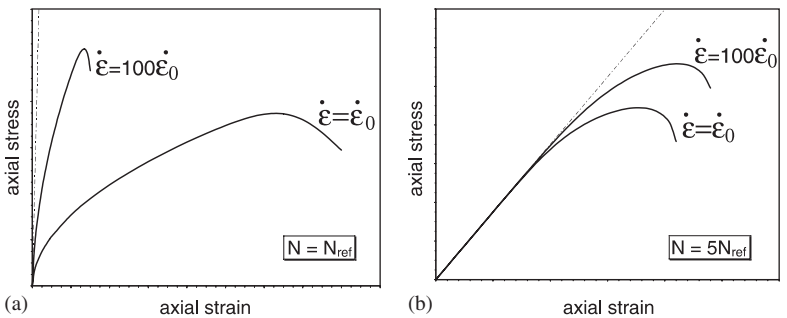

Figure 3. Axial stress versus axial strain for different strain rates (quasistatic tests): (a) low value of viscosity exponent; and (b) high value of viscosity exponent ($N = 5N_{\text{ref}}$).

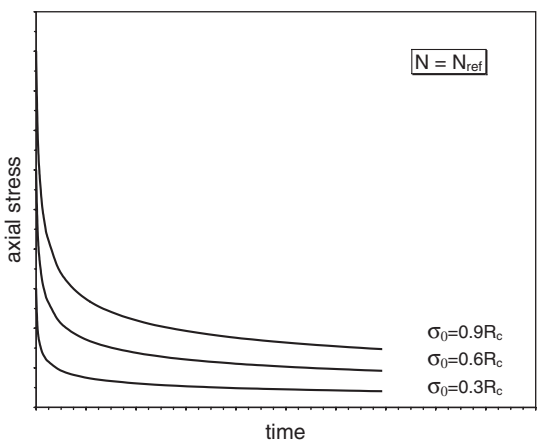

Figure 4. Axial stress versus time for different initial stresses (relaxation tests).

For the creep test, simulations were run with two loading levels ($\sigma = \sigma_0$ and $\sigma = 1.5\sigma_0$). It was found that, for a high value of N ($N = 5N_{\text{ref}}$), the stress has considerable influence on the axial inelastic strain (Figure 2(b)), whereas, conversely, when N is small ($N = N_{\text{ref}}$), the difference is less marked (Figure 2(a)).

Under monotonous compressive loading (Figure 3) a low value of the viscosity exponent leads to a significant influence of the loading strain rate (Figure 3(a)). Axial strains increase with reduction in $\dot{\varepsilon}$. On the other hand, for a high value of N (Figure 3(b)) the influence of loading rate on the amplitude of viscoplastic strains is much less marked. In comparison, elastic strains are represented on the same figure by a dotted line.

For a high value of N, the relaxation test simulations (Figure 4) give evidence of the considerable influence of initial axial stress. At low levels of imposed initial stress ($\sigma_0 = 0.3R_c$ or $0.6R_c$) stress relaxation is virtually non-existent.

In summary, the main role of the viscosity exponent N is to express the sensitivity of the growth of viscous strains to a stress variation. The experiment shows that the value of N varies between 2 and about 100 (2 for highly viscous materials and 100 for materials of low viscosity). A very high value of N suggests the application of an elasto-plastic law.

3.2.2. Strain-hardening parameter M. The parameter M expresses an increase in strength as a result of strain-hardening. The analysis of the strain-hardening parameter, M, is presented in Figure 5. Generally speaking, it is found that a low value of this variable causes viscoplastic strains appear rapidly, reaching higher values than those obtained with a higher strain-hardening parameter. This is visible in creep conditions on Figure 5(a). The same trend is observed under monotonous compression on Figure 5(b) where the elastic strain has been plotted (dotted line).

In relaxation (Figure 5(c)), a rapid fall in stress is observed for a low strain-hardening parameter, whereas a higher value leads to a slower decrease in stress. After the first relaxation phase, the slope of the curve no longer appears to be sensitive to the quantity M. Practically, M varies from 2 to about 50.

3.2.3. Viscoplastic stiffness K. The influence of the viscoplastic stiffness coefficient K on the model response is illustrated in Figure 6. In a similar manner to the observations for the strain-hardening parameter, M, it is found that irreversible strains become all the greater as K becomes

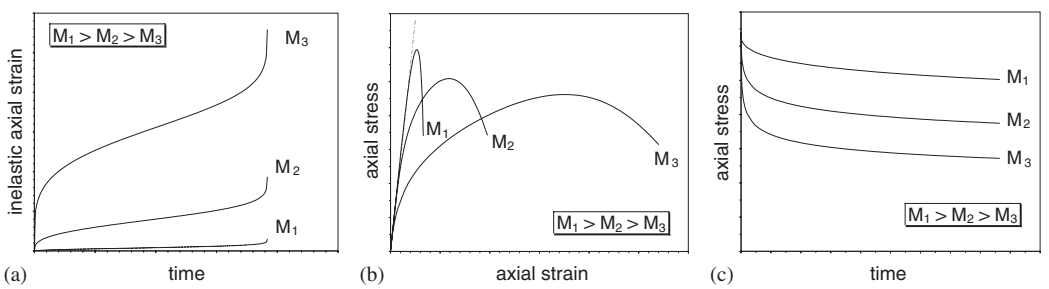

Figure 5. Influence of the work hardening parameter, M: (a) inelastic axial strain versus time for different values (creep tests); (b) axial stress versus axial strain for different strain rates (quasistatic tests); and (c) axial stress versus time for different stresses (relaxation tests).

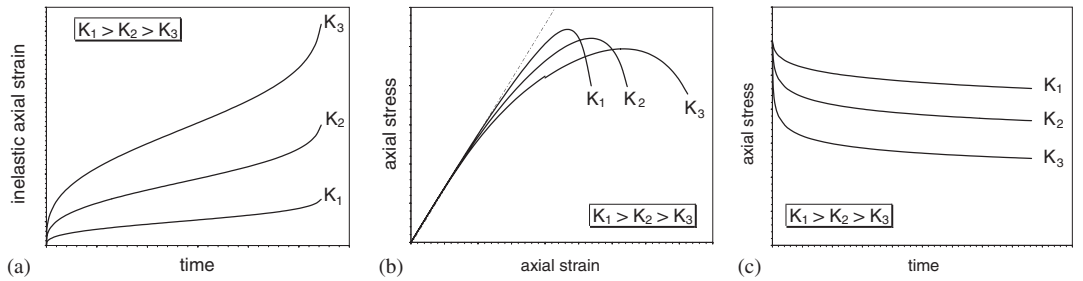

Figure 6. Influence of the viscoplastic stiffness coefficient, K: (a) inelastic axial strain versus time for different values (creep tests); (b) axial stress versus axial strain for different strain rates (quasistatic tests); and (c) axial stress versus time for different stresses (relaxation tests).

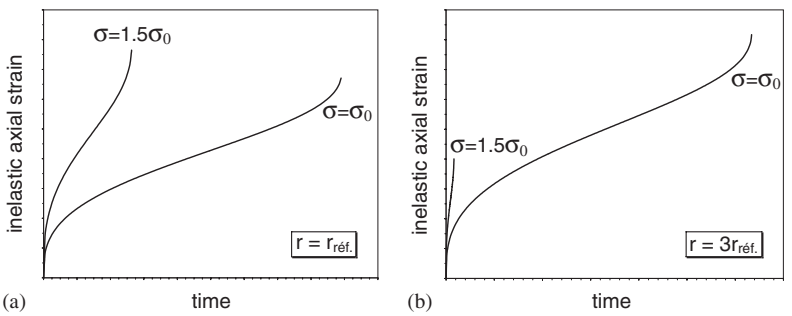

Figure 7. Inelastic axial strain versus time for different stresses (creep tests): (a) low value of damage exponent ($r = r_{\text{ref}}$); and (b) high value of damage exponent ($r = 3r_{\text{ref}}$).

smaller. This is applicable in creep (Figure 6(a)), in monotonous strain-controlled compression (Figure 6(b)) and in relaxation tests (Figure 6(c)).

The main difference between the effect of the parameter M and that of the parameter K is that the viscoplastic stiffness coefficient has no influence on the shape of the curves, but provides only a quantitative adjustment. For rocks, its value ranges from 50 to 10 000 MPa s.

3.2.4. Damage exponent r. The sensitivity of the model to variations in the damage exponent, r, is presented in Figures 7 and 8. In a similar manner to the procedure followed for the analysis of the viscosity exponent, N, different values of the test parameters (imposed creep stress, σ, imposed loading rate under monotonous compression, $\dot{\varepsilon}$, and initial stress in relaxation, σ_0) were examined. Two different values of r were studied.

The creep curves (Figure 7) reflect a clear dependence of imposed stress level as a function of the damage exponent. For a high value of r, failure occurs very soon after the stress application (Figure 7(b)). The axial inelastic strain on failure is lower for $\sigma = 1.5\sigma_0$ than that obtained for $\sigma = \sigma_0$. The smaller the damage exponent, the less sensitive the model becomes to a variation instress level (Figure 7(a)).

The monotonous strain-controlled loading tests (Figure 8) show that the peak values on the axial stress–axial strain curve are sensitive to the loading rate for a low damage exponent value.

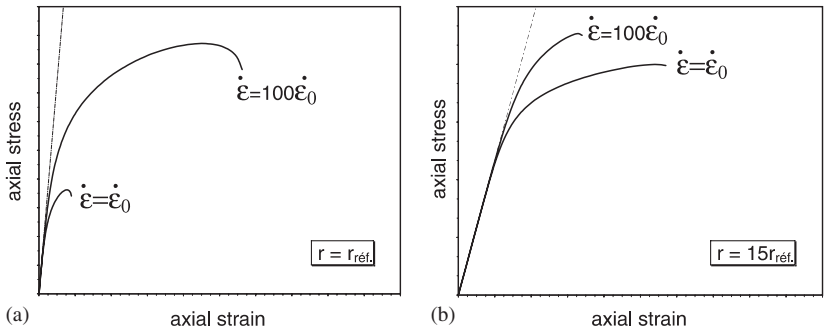

Figure 8. Axial stress versus axial strain for different strain rates (quasistatic tests): (a) low value of damage exponent ($r = r_{\text{ref}}$); and (b) high value of damage exponent ($r = 15r_{\text{ref}}$).

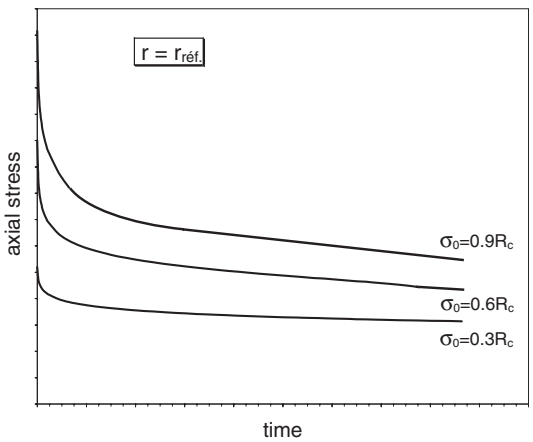

Figure 9. Axial stress versus time for different stresses (relaxation tests): (a) low value of damage exponent ($r = r_{\text{ref}}$); and (b) high value of damage exponent ($r = 15r_{\text{ref}}$).

Conversely, by increasing the value of r, a less marked sensitivity to variations in $\dot{\varepsilon}$ can be modelled (Figure 8(a)).

The simulation of a relaxation test (Figure 9) indicates that a smaller damage exponent leads to greater stress relaxation. Conversely, with a higher value of r the relaxation is less significant, especially when a low initial stress is imposed ($\sigma_0 = 0.3\sigma_c$).

In addition, a highly accelerated rise in the damage variable was observed for a high value of r whereas a lower value generates a slower expansion. The time required to reach failure ($D = 1$) increases when r becomes smaller. The parameter r in the model therefore reflects the dependence of the expansion of the damage variable on a stress variation. Its role is therefore similar to that of parameter N in viscoplasticity.

3.2.5. Damage progression parameter q. The analysis of the damage progression parameter, q, is shown in Figure 10. The role of this parameter in the model can be easily identified for each loading configuration. As a general rule, q can be said to be responsible for the variation in the

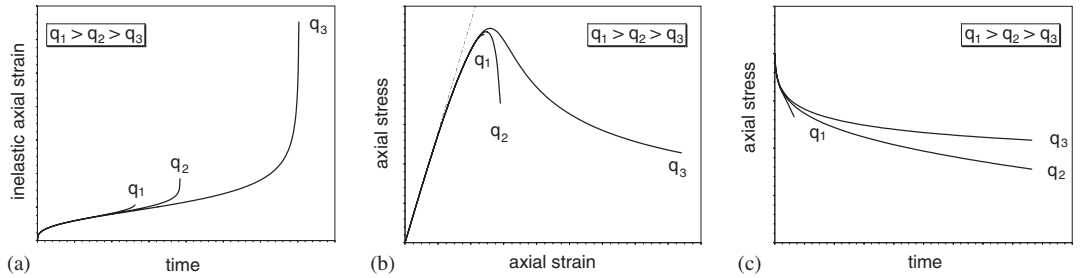

Figure 10. Influence of the damage progression parameter q: (a) inelastic axial strain versus time for different values (creep tests); (b) axial stress versus axial strain for different strain rates (quasistatic tests); and (c) axial stress versus time for different stresses (relaxation tests).

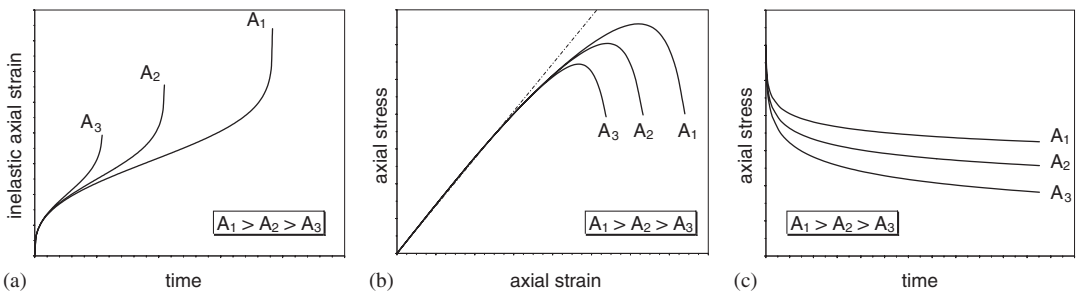

Figure 11. Influence of the tenacity coefficient A: (a) inelastic axial strain versus time for different values (creep tests); (b) axial stress versus axial strain for different strain rates (quasistatic tests); and (c) axial stress versus time for different stresses (relaxation tests).

rate of change of the damage variable, i.e. the greater the value of q the more quickly the damage expands and the more sudden failure occurs. Conversely, a lower value of q leads to a delayed, less brittle failure.

For example, in creep (Figure 10(a)) a high damage expansion parameter leads to sudden failure which is reflected in an almost total absence of the tertiary phase. As the value of q reduces, this phase becomes more distinct and a high axial inelastic strain can be observed before failure.

The same trend is noted in monotonous strain-controlled compression (Figure 10(b)). As the parameter q decreases, the post-peak phase becomes increasingly significant and the model describes a more ductile behaviour. Conversely, a high value of q leads to brittle failure, without strain-softening.

The simulation of relaxation tests (Figure 10(c)) shows that as the value of the damage expansion parameter decreases, the damage continues to expand in a relaxation regime. This leads to a more significant drop in stress and may possibly cause failure in relaxation conditions.

3.2.6. Tenacity coefficient A. We shall now examine the influence of the tenacity coefficient A on the model response to different loading configurations (Figure 11). The role played by A in the damage process is comparable to that played by the coefficient K in viscoplastic conditions. The parameters K and A are used for quantitative adjustment of the values.

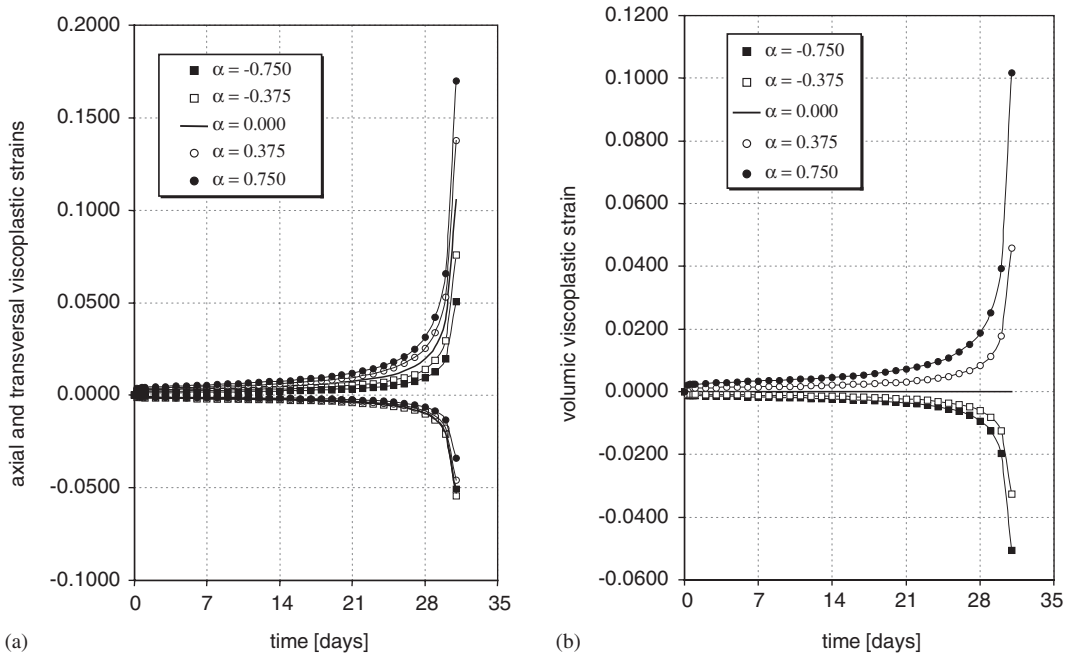

Figure 12. Simulations of creep tests in uniaxial compression for anisotropic damage, $\beta = 1$: (a) axial and transversal strains; and (b) volumetric strain.

For example, in creep conditions (Figure 11(a)) different times to failure correspond to different A, while keeping the same axial inelastic strain expansion value. Under quasi-static strain-controlled compression (Figure 11(b)) the tenacity coefficient affects the amplitude of the axial strain caused by damage. It can clearly be seen that viscous axial strain is the same (deviation of the curves with respect to the elastic line is identical) for the three values of A before the stress reaches the level where the damage effect becomes significant. On the relaxation curve (Figure 11(c)), the increase in tenacity coefficient slows down the stress reduction but the change in σ has the same general trend.

The parameter, A, thus allows the failure time to be adjusted without changing the shape of the curve $D(t)$. The higher the value of A the longer it takes for failure to occur. It can therefore be said that the parameter A reflects the damage resistance in the model. The parameter A is expressed in (MPa s), the other damage parameters (r and q) are dimensionless.

3.2.7. Viscoplastic dilatancy parameter α *and damage anisotropy parameter* β. Finally, the influences of the viscoplastic dilatancy parameter, α and damage anisotropy parameter, β are shown. These two parameters, which represent an enhancement of the classic Lemaitre model, are directly responsible for the dilatancy of irreversible volumetric strains.

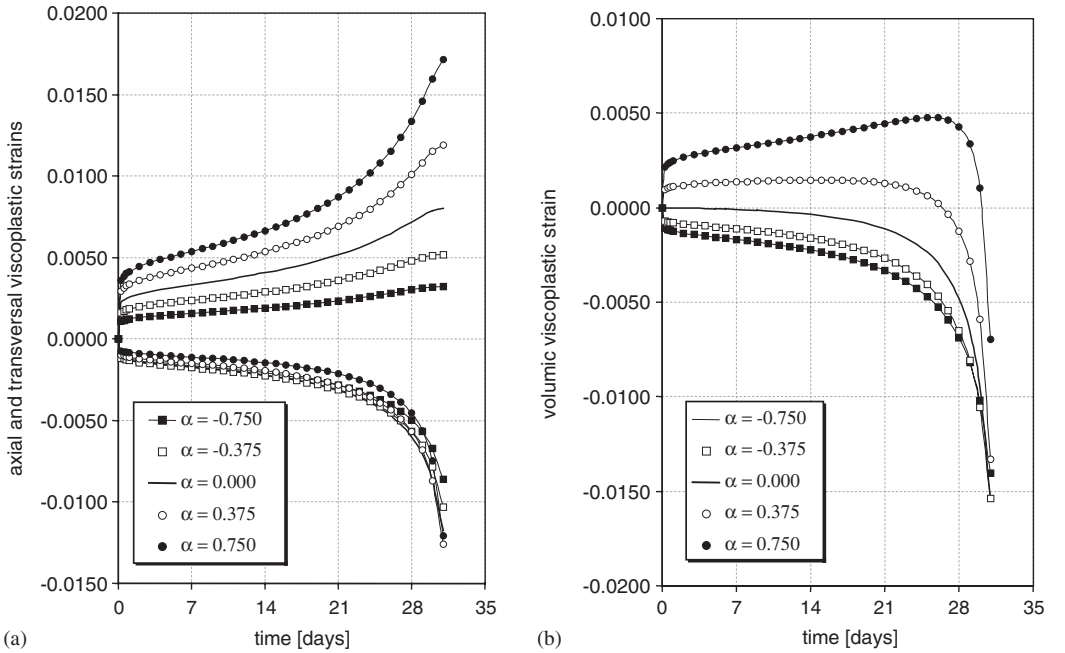

Figure 13. Simulations of creep tests in uniaxial compression for anisotropic damage, $\beta = 0.5$: (a) axial and transversal strains; and (b) volumetric strain.

The general cases of anisotropy were modelled by varying the values of β between 0 and 1 in 0.5 steps. The values of α sweep a range from -0.75 to 0.75 in 0.375 steps. The results of creep test simulations are presented in Figures 12–14. Depending on these two parameters, the delayed volumetric strain can be purely contracting, purely dilatant or a combination of both, i.e. contracting first and then dilatant.

For isotropic damage ($\beta = 1$), simultaneous failure is observed in the axial and lateral directions (Figure 12). As the value of β decreases, damage becomes increasingly anisotropic and the tertiary creep phase in the axial direction gradually attenuates. For $\beta = 0$, damage expands only in the direction perpendicular to the applied stress direction (Figure 14).

The simulations of strain-controlled loading tests are represented in Figures 15–17. The set of parameters applied here was the same as for the creep test simulation.

It is worth noting that, for a completely anisotropic damage expansion ($\beta = 0$, Figure 15), the behaviour is of the brittle type. This phenomenon is due to the 'latent' variation in damage in the lateral direction, leading to failure but is not reflected on the axial curves. With the progressive reduction in anisotropy (increase in value of β) behaviour becomes ductile with an increasingly marked post-peak phase.

Note that the uniqueness of the solution is not lost because each point of a curve corresponds to a particular state of the material characterized by a time-dependent expanding damage state.

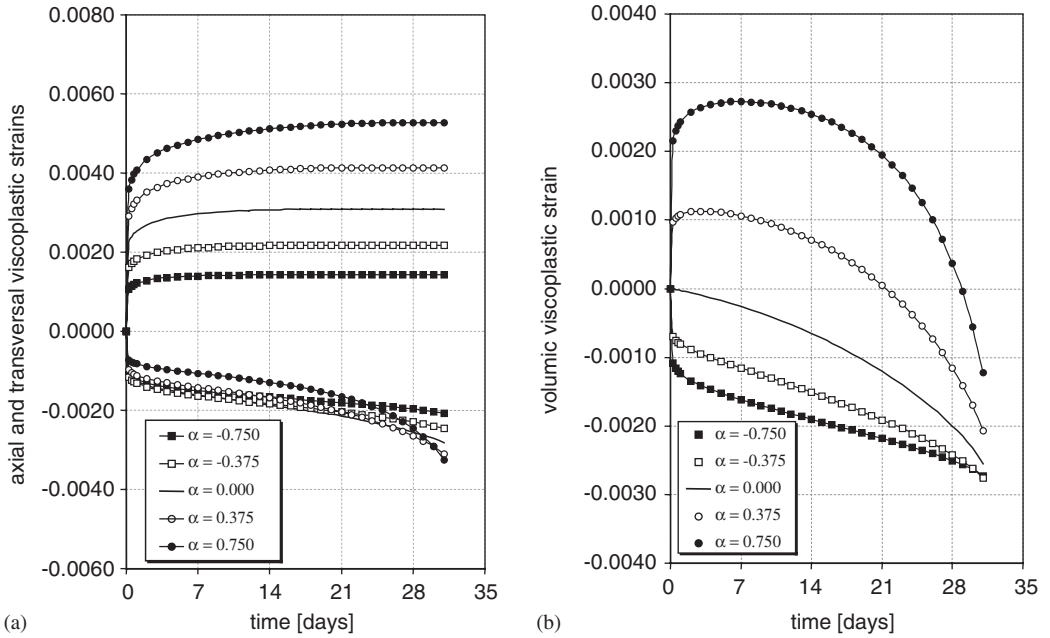

(Applied stress : 25 MPa ; M=1.5 ; N=15 ; K=5000 MPa.s; q=0.05 ; r=5 ; A=525 MPa.s)

Figure 14. Simulations of creep tests in uniaxial compression for isotropic damage, $\beta = 0$: (a) axial and transversal strains; and (b) volumetric strain.

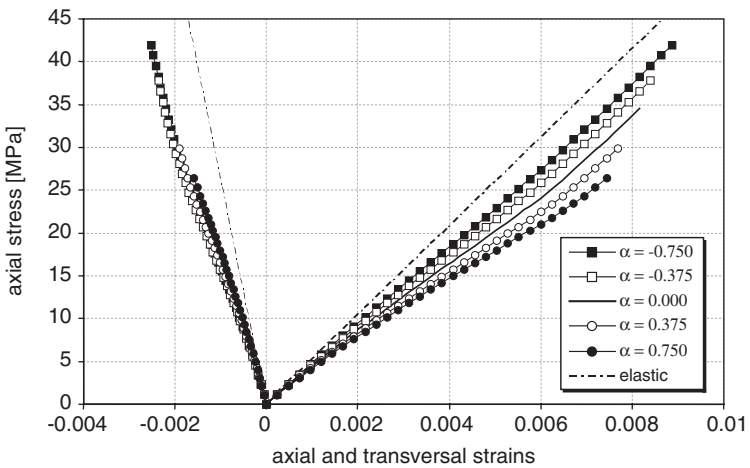

(Loading rate : 10^{-6} s^{-1} ; M=1.5 ; N=15 ; K=5000 MPa.s; q=0.05 ; r=5 ; A=525 MPa.s)

Figure 15. Simulations of quasistatic tests in uniaxial compression for isotropic damage, $\beta = 0$. Axial stress versus axial and transversal strains.

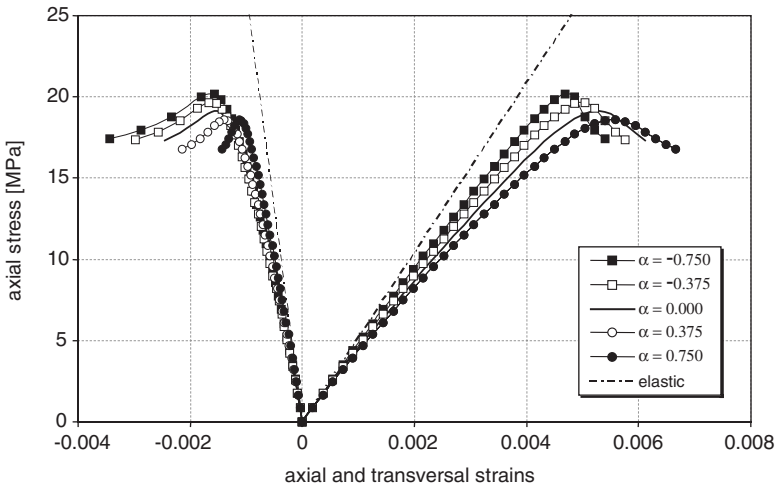

Figure 16. Simulations of quasistatic tests in uniaxial compression for anisotropic damage, $\beta = 0.5$. Axial stress versus axial and transversal strains.

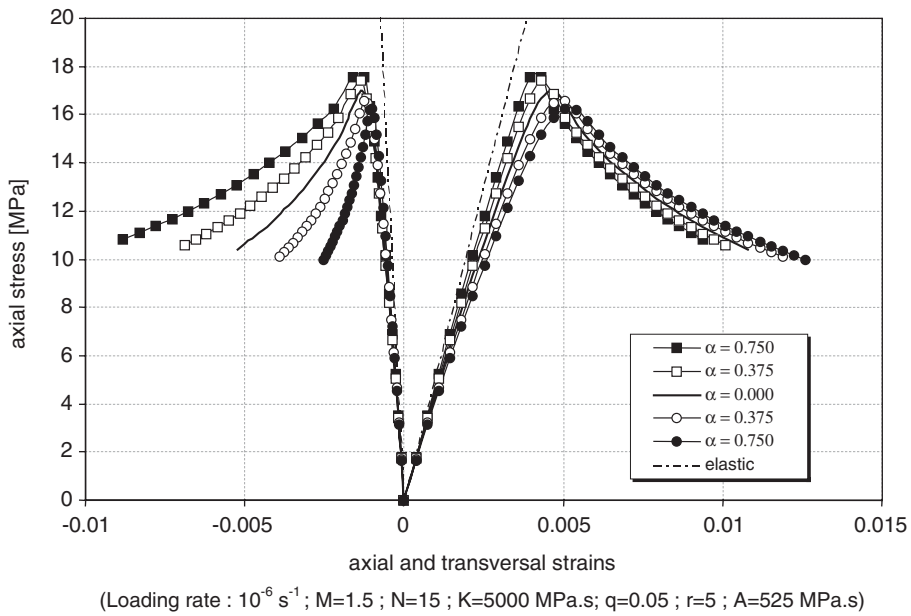

Figure 17. Simulations of quasistatic tests in uniaxial compression for anisotropic damage, $\beta = 1$. Axial stress versus axial and transversal strains.

4. COMPARISON WITH TEST RESULTS

In this section, the performance of the viscoplastic-damage model is assessed by comparison with the results of tests carried out on a variety of rocks. However, it is rare to have access to complete experimental data bases with the results of creep, relaxation and quasi-static compressions tests on the same material. Consequently, the aim of the analysis presented in the following section is not to determine a set of unique parameters for each material studied, but rather to illustrate the capacity of the model to take into account and reproduce the various phenomena brought to light by the laboratory tests.

4.1. Creep test in uniaxial compression

4.1.1. Test on an argillite. By performing a creep test on an argillite [29], the rate of change in volume was highlighted. Under a uniaxial stress of 26 MPa, the rock shows delayed volumetric behaviour: contracting at the start of the test but subsequently dilating (Figure 18). The first phase lasts for about ten days and leads to a reduction in sample volume. There then follows a change in the volumetric behaviour trend; contraction of the sample is replaced by expansion (i.e. dilatancy). After 270 days, the sample has the same volume as it had initially before stress application. From this time onwards, behaviour is generally dilating. This reversal of trend could possibly be explained by a combination of contracting viscous behaviour and dilating anisotropic damage. However, no information is available regarding the delayed failure of the rock.

In order to determine the intrinsic viscoplastic parameters of the materials, the analysis was limited to the first week of the test, i.e. the period during which delayed damage has not yet been

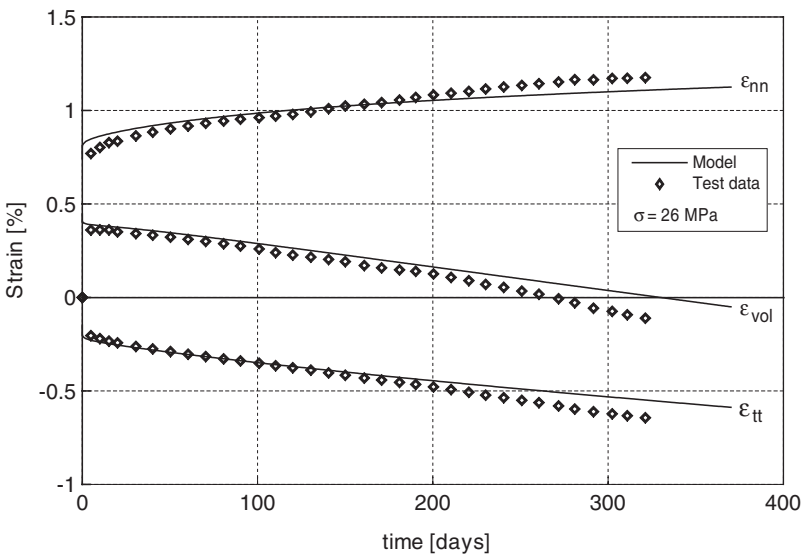

E=3500 MPa, ν = 0.2, N=25, M=3.17, K=440MPa.s, α=-0.5, r =11.3, q=0.25, A=115.5Pa.s, β=0.5

Figure 18. Comparison between the strains–time curves obtained from the model and experimentally from a creep test performed on argillite.

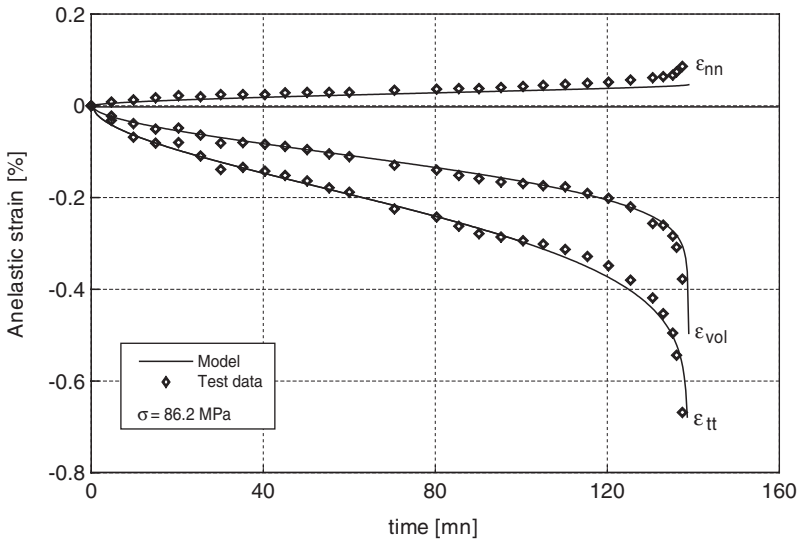

N=10, M=12, K=212MPa.s, α=-2.15, r =10, q=0.59, A=274Pa.s, β=0.5

Figure 19. Comparison between the strains–time curves obtained from the model and experimentally from a creep test performed on marble, Singh [2].

able to exert a significant influence on the change in material strain. For the damage parameters, the procedure followed is that proposed by Hajdu [19]. Figure 18 compares the experimental results with those obtained by the model. There is a very good approximation of the strain induced by the uniaxial stress in the rock. The viscoplastic model, making allowance for delayed volumetric strains, proves to be particularly well suited to modelling the complex delayed mechanical behaviour of the argillite sample.

Concerning the two new parameters introduced, namely α and β, it is worth noting that the values obtained imply anisotropic damage with dilatancy.

4.1.2. Test on a marble. Another experimental result, obtained with uniaxial creep on a sample of Sicilian marble, as reported by Singh [2], was simulated by means of the model. The model parameters setting method is similar to that used for argillite. The parameters were calibrated with respect to the experimental points. Figure 19 shows the results obtained.

By examining the parameters governing the change in volume, a very high negative coefficient of viscoplastic expansion is noted. This result was expected, because the porosity of a rock such as marble is very low and, as a result, it does not show a contracting phase due to micropore collapse. On the other hand, the value of the anisotropic damage parameter, β, shows the anisotropy of damage.

4.2. Quasi-static test in uniaxial compression

4.2.1. Test on an anhydrite. One result of the tests conducted on an anhydrite is presented in Figure 20. The delayed behaviour under creep is similar to that of the argillite and shows

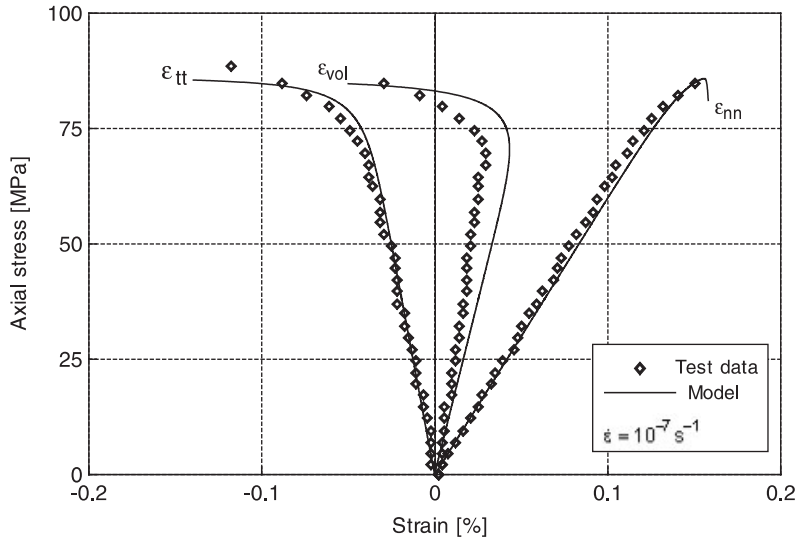

E=60 GPa, ν=0.3, N=10, M=75, K=2100 MPa.s, α=-0.5, r=10; q=0.25, A=165MPa.s, β=0.25

Figure 20. Comparison between the stress–strains curves obtained from the model and experimentally from strain-controlled compression test performed on anhydrite.

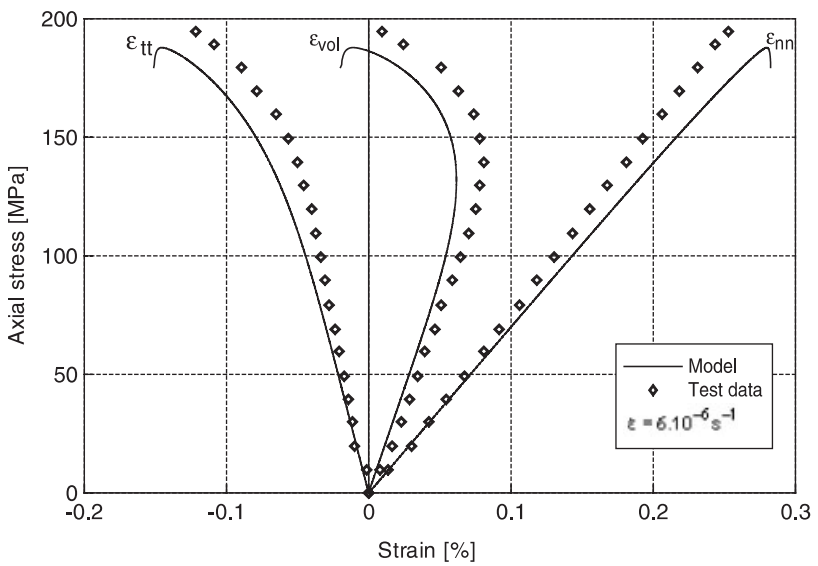

E=70 GPa, ν=0.3, N=10, M=10, K=255MPa.s, α=-2.5, r=10; q=0.75, A=370MPa.s, β=0.25

Figure 21. Comparison between the stress–strains curves obtained from the model and experimentally from monotonic compression test performed on granite [30].

a contracting phase followed by a dilating phase under a sufficiently high uniaxial stress. A negative value for α was fixed. As for the value of β, the transverse strain is clearly greater than the axial strain when the maximum stress is applied thus reflecting a pronounced anisotropy of damage. Figure 20 shows the model reproduction of this test.

4.2.2. Test on a granite. The last example is also taken from the literature and concerns uniaxial compression on a sample of granite taken from Lac de Bonnet [30].

Observations show that inelastic delayed strains also appear in brittle rocks, even at stress values that may be considered low compared to the strength of the material. The delayed growth of a micro-crack can thus be considered as a viscoplastic process, thereby justifying the application of the model. Figure 21 compares the experimental results with those obtained with the model. Particularly noteworthy is the very high negative value of the parameter α. This value is very close to that obtained when making the calibration on the creep curve of the Sicilian marble.

5. CONCLUSIONS

The model presented in this paper was developed to model time dependent behaviour of rock including delayed failure. The inclusion of the Drucker–Prager yield surface in the Lemaitre viscoplastic constitutive equation showed the ability of the model to exhibit dilatancy and contractancy associated with viscoplastic strain. Moreover, the introduction of a second rank tensor for damage parameters allowed one to reproduce anisotropic damage observed in compression tests, either creep tests, relaxation tests or quasistatic strain-controlled tests.

The model requires ten parameters. A parametric study was presented to highlight the influence of each of them as well as their physical significance. Some comparisons with test results such as creep tests or strain-controlled compression tests showed a good prediction of the mechanical responses, especially for time to failure.

This constitutive model has been used in finite element simulations of highly non-homogeneous problems like for the prediction of the evolution in time of the EDZ around underground openings, planned for radioactive waste repositories. In this zone, due to the damaging process, dilatancy and porosity increase and can create possible preferential pathways for radionuclide migration. This model is capable of simulating these phenomena.

APPENDIX A

Details of the new model presented in the text are given here for the case of uniaxial loading. An axisymmetrical reference frame is considered, which allows the loading axis, noted 1, to be the axis of revolution.

The stress tensor

$$\boldsymbol{\sigma} = \begin{bmatrix} \sigma_1 & 0 & 0 \\ 0 & 0 & 0 \\ 0 & 0 & 0 \end{bmatrix} \tag{A1}$$

The effective stress tensor

$$\tilde{\boldsymbol{\sigma}} = \begin{bmatrix} \dfrac{\sigma_1}{1-D_1} & 0 & 0 \\ 0 & 0 & 0 \\ 0 & 0 & 0 \end{bmatrix} \tag{A2}$$

The effective deviator

$$\tilde{\mathbf{S}} = \frac{\sigma_1}{1-D_1} \begin{bmatrix} \frac{2}{3} & 0 & 0 \\ 0 & -\frac{1}{3} & 0 \\ 0 & 0 & -\frac{1}{3} \end{bmatrix} \tag{A3}$$

and the tensor $\tilde{\tilde{\mathbf{S}}}$

$$\tilde{\tilde{\mathbf{S}}} = \begin{bmatrix} \dfrac{2}{3}\dfrac{\sigma_1}{(1-D_1)(1-D_1)} & 0 & 0 \\ 0 & -\dfrac{1}{3}\dfrac{\sigma_1}{(1-D_1)(1-D_3)} & 0 \\ 0 & 0 & -\dfrac{1}{3}\dfrac{\sigma_1}{(1-D_1)(1-D_3)} \end{bmatrix} \tag{A4}$$

as well as the mean effective stress

$$\tilde{\sigma}_{\mathrm{m}} = \frac{1}{3}\frac{\sigma_1}{1-D_1} \tag{A5}$$

and the equivalent effective stress

$$\tilde{\sigma}_{\mathrm{eq}} = \frac{\sigma_1}{1-D_1} \tag{A6}$$

thus enabling the expression strain rate to be written in the following forms. For the axial direction

$$\dot{\varepsilon}_1^{\mathrm{vp}} = \frac{1}{1-D_1}\left(1+\frac{\alpha}{3}\right)\left(\frac{(1+(\alpha/3))\sigma_1}{(1-D_1)Kp^{1/M}}\right)^N \tag{A7}$$

and for the transversal direction

$$\dot{\varepsilon}_3^{\mathrm{vp}} = \frac{1}{1-D_3}\left(-\frac{1}{2}+\frac{\alpha}{3}\right)\left(\frac{(1+(\alpha/3))\sigma_1}{(1-D_1)Kp^{1/M}}\right)^N \tag{A8}$$

The strain-hardening scalar, p, is then calculated

$$\left\| \left(\frac{3}{2}\frac{\tilde{\tilde{\mathbf{S}}}}{\tilde{\sigma}_{\mathrm{eq}}} + \frac{\alpha(\mathbf{I}-\mathbf{D})^{-1}}{3} \right) \right\| = \sqrt{\left(\frac{1+\alpha/3}{1-D_1}\right)^2 + 2\left(\frac{-1/2+\alpha/3}{1-D_3}\right)^2} \tag{A9}$$

$$p = \sqrt{\frac{2}{3}}\dot{\varepsilon}_1^{\mathrm{vp}} \frac{\sqrt{\left(\dfrac{1+\alpha/3}{1-D_1}\right)^2 + 2\left(\dfrac{-1/2+\alpha/3}{1-D_3}\right)^2}}{\dfrac{1+\alpha/3}{1-D_1}} \tag{A10a}$$

and

$$p = \sqrt{\frac{2}{3}}\dot{\varepsilon}_3^{\mathrm{vp}} \frac{\sqrt{\left(\dfrac{1+\alpha/3}{1-D_1}\right)^2 + 2\left(\dfrac{-1/2+\alpha/3}{1-D_3}\right)^2}}{\dfrac{-1/2+\alpha/3}{1-D_3}} \tag{A10b}$$

The expression of time-dependent viscoplastic strain, under constant loading (creep test) is then obtained by integration of expressions (A7) and (A8)

$$\varepsilon_1^{\mathrm{vp}}(t) = \left(1+\frac{\alpha}{3}\right)\left\{\frac{M+N}{M}\left(\frac{(1+\alpha/3)\sigma_1}{K}\right)^N \int_0^t \left(\frac{1}{1-D_1}\right)^{M+N/M} \times \left(\frac{1}{1-D_1}\left[\frac{2}{3}\left(\frac{1+\alpha/3}{1-D_1}\right) + \frac{4}{3}\left(\frac{-1/2+\alpha/3}{1-D_3}\right)\right]^{-1/2M}\right)^N \mathrm{d}t\right\}^{M/M+N} \tag{A11a}$$

and

$$\varepsilon_3^{\mathrm{vp}}(t) = \left(-\frac{1}{2}+\frac{\alpha}{3}\right)\left\{\frac{M+N}{M}\left(\frac{(1+\alpha/3)\sigma_1}{K}\right)^N \int_0^t \left(\frac{1}{1-D_3}\right)^{M+N/M} \times \left(\frac{1}{1-D_1}\left[\frac{2}{3}\left(\frac{1+\alpha/3}{1-D_1}\right) + \frac{4}{3}\left(\frac{-1/2+\alpha/3}{1-D_3}\right)\right]^{-1/2M}\right)^N \mathrm{d}t\right\}^{M/M+N} \tag{A11b}$$

where the change in damage variables is expressed by

$$\dot{D}_3 = \left(\frac{\sigma_1}{A(1-D_3)^{2q}}\right)^r \tag{A12a}$$

$$\dot{D}_1 = \beta\left(\frac{\sigma_1}{A(1-D_1)^{2q}}\right)^r \tag{A12b}$$

and is written in integrated form (with the conditions $\sigma_1 = \text{constant}$ and $D_1 = D_3 = 0$ at $t = 0$)

$$1 - D_3 = \left[1 - (2qr+1)\left(\frac{\sigma_1}{A}\right)^r t\right]^{1/2qr+1} \tag{A13a}$$

$$1 - D_1 = \left[1 - \beta(2qr+1)\left(\frac{\sigma_1}{A}\right)^r t\right]^{1/2qr+1} \tag{A13b}$$

These equations cannot be solved analytically. The simulations of a creep test and a quasi-static test were programmed in Fortran language, and the integration method used a constant time step. However, it is possible to obtain an analytical solution in the case of a creep test with isotropic damage ($\beta = 1$). The integrated form of the behaviour law is then expressed by

$$\varepsilon_1^{\mathrm{vp}}(t) = \left(1 + \frac{\alpha}{3}\right)\left\{ t_{\mathrm{rupt}} \frac{A}{B}\left[1 - \left(1 - \frac{t}{t_{\mathrm{rupt}}}\right)^{B}\right]\left[\frac{(1 + (\alpha/3))\sigma_1}{K\left(\frac{2}{9}\alpha^2 + 1\right)^{1/2M}}\right]^{N}\right\}^{1/A} \tag{A14a}$$

$$\varepsilon_3^{\mathrm{vp}}(t) = \left(-\frac{1}{2} + \frac{\alpha}{3}\right)\left\{ t_{\mathrm{rupt}} \frac{A}{B}\left[1 - \left(1 - \frac{t}{t_{\mathrm{rupt}}}\right)^{B}\right]\left[\frac{(1 + (\alpha/3))\sigma_1}{K\left(\frac{2}{9}\alpha^2 + 1\right)^{1/2M}}\right]^{N}\right\}^{1/A} \tag{A14b}$$

with

$$A = \frac{M + N}{M} \tag{A15}$$

$$B = \frac{2qr - N}{2qr + 1} \tag{A16}$$

and t_{rupt} the time to failure

$$t_{\mathrm{rupt}} = \frac{1}{2qr + 1}\left(\frac{\sigma_1}{A}\right)^{-r} \tag{A17}$$

For the monotonous loading case, the stress is expressed as a function of viscoplastic strain for an imposed constant axial strain rate. The elastic and viscoplastic mechanisms can no longer be separated as in the creep test because a total strain rate is imposed and damage affects not just the viscoplastic component of strain but also the elastic component, i.e.

$$\dot{\varepsilon}_1^{\mathrm{tot}} = \dot{\varepsilon}_1^{\acute{\mathrm{e}}} + \dot{\varepsilon}_1^{\mathrm{vp}} = cste \tag{A18}$$

where

$$\dot{\varepsilon}_1^{\acute{\mathrm{e}}} = \frac{\dot{\sigma}_1}{(1 - D_1)E} \tag{A19}$$

Therefore we can write

$$\dot{\varepsilon}_1^{\mathrm{tot}} = C^{\mathrm{te}} = \frac{\dot{\sigma}_1}{(1 - D_1)E} + \frac{1}{1 - D_1}\left(1 + \frac{\alpha}{3}\right)\left(\frac{(1 + (\alpha/3))\sigma_1}{(1 - D_1)Kp^{1/M}}\right)^{N} \tag{A20}$$

with

$$p = \sqrt{\frac{2}{3}}\left(C^{\mathrm{te}}t - \frac{\sigma_1}{(1 - D_1)E}\right)\frac{\sqrt{((1 + \alpha/3)/1 - D_1)^2 + 2((-1/2 + \alpha/3)/1 - D_3)^2}}{(1 + \alpha/3)/1 - D_1} \tag{A21}$$

The stress increments, $d\boldsymbol{\sigma}_1$, were calculated numerically for each time step, dt. The lateral strain is then obtained for each step by substitution of the values σ_1, D_1, D_3 in

$$d\varepsilon_3^{vp} = -\frac{v\,d\sigma_1}{(1-D_1)E} + \frac{1}{1-D_3}\left(-\frac{1}{2}+\frac{\alpha}{3}\right)\left(\frac{(1+(\alpha/3))\sigma_1}{(1-D_1)Kp^{1/M}}\right)^N \tag{A22}$$

REFERENCES

1. Cristescu ND, Hunsche U. *Time Effect in Rock Mechanics*. Wiley: New York, 1998; 342.
2. Singh DP. A study of creep of rocks. *International Journal of Rock Mechanics and Mining Sciences and Geomechanics Abstracts* 1975; **12**:271–276.
3. Lockner DA. Room temperature creep in saturated granite. *Journal of Geophysical Research* 1993; **98**:475–487.
4. Scholz CH. Mechanism of creep in brittle rock. *Journal of Geophysical Research* 1968; **73**:3295–3302.
5. Dusseault MB, Fordham CJ. Time-dependent behavior of rocks. In *Comprehensive Rock Engineering*, Hudson JA (ed.), vol. 3. Pergamon Press: Oxford, 1993; 119–149.
6. Tapponier P, Brace WF. Development of stress-induced microcracks in Westerly granite. *International Journal of Rock Mechanics and Mining Sciences and Geomechanics Abstracts* 1976; **13**:103–112.
7. Gatelier N, Pellet F, Loret B. Mechanical damage of an anisotropic rock under cyclic triaxial tests. *International Journal of Rock Mechanics and Mining Sciences* 2002; **39**(3):335–354.
8. Boidy E, Pellet F. Identification of mechanical parameters for modeling time-dependent behavior of shale. *Workshop Andra*, Paris, France. Balkema: Rotterdam, 2000; 11–22.
9. Ghoreychi M, Berest P, Hardy HR, Langer M. The mechanical behaviour of salt. *Proceedings of the 3rd Conference on Rock Salt*, Chapter I. Trans. Tech. Publications (TTP): Paris, 1993.
10. Aubertin M, Simon R. A damage initiation criterion for low porosity rocks. *International Journal of Rock Mechanics and Mining Sciences* 1997; **34**(3–4):554.
11. Munson DE. Constitutive model of creep in rock salt applied to underground room closures. *International Journal of Rock Mechanics and Mining Sciences* 1997; **34**(2):233–247.
12. Pellet F, Hajdu A, Boulon M, Deleruyelle F, Besnus F. Numerical modeling of underground structures taking into account the visco-plastic behavior and damaging of rock. *Proceedings of the International Conference on Numerical Models in Geomechanics-NUMOG VIII*, Roma-Italy, 2002; 399–404.
13. Pellet F, Zerfa FZ, Hajdu A, Deleruyelle F, Besnus F. Numerical modelling of the excavated damaged zone around underground openings. *Proceedings of the 3rd Asian Rock Mechanics Symposium*, vol. 1, Kyoto, Japan, 2004; 727–732.
14. Lemaitre J, Chaboche J-L. Aspect phénoménologique de la rupture par endommagement. *Journal de Mécanique Appliquée* 1978; **2**(3):317–365.
15. Perzyna P. Fundamental problems in viscoplasticity. *Advances in Applied Mechanics* 1966; **9**:247–377.
16. Drucker DC, Prager W. Soil mechanics and plastic analysis or limit design. *Quarterly of Applied Mathematics* 1952; **10**:157–165.
17. Desrues J. Limitations du choix de l'angle de frottement pour le critère de plasticité de Drucker-Prager. *Revue Française de Génie Civil* 2002; **6**:853–862.
18. Carioso A, Willam K, Etse G. On the consistency of viscoplastic formulations. *International Journal of Solids and Structures* 2000; **37**:7349–7369.
19. Hajdu A. Modélisation numérique du comportement viscoplastique endommageable des roches et application aux ouvrages souterrains de stockage. *Thèse de doctorat de* l'Université Joseph Fourier, Grenoble I, 2003; 333.
20. Betten J. Damage tensors in continuum mechanics. *Journal de Mécanique Théorique and Appliquée* 1983; **2**(1):13–32.
21. Shao JF, Rudnicki JW. A microcrack based continuous damage model for brittle geomaterials. *Mechanics of Materials* 2000; **32**:607–619.
22. Chaboche JL. Le concept de contrainte effective appliqué à l'élasticité et à la viscoplasticité en présence d'un endommagement anisotrope. In *Colloques Internationaux du CNRS*, *Euromech 115*, Boehler JP (ed.), Villard de Lens, France, 19–22 June 1979; 737–759.
23. Zheng Q-S, Betten J. On damage effective stress and equivalence hypothesis. *International Journal of Damage Mechanics* 1996; **5**:219–240.
24. Sidoroff F. Description of anisotropic damage application to elasticity. In *Symposium IUTAM*, Hult J, Lemaitre J (eds), Senlis, France, 27–30 May 1980; 237–244.
25. Cordebois J-P, Sidoroff F. Endommagement anisotrope en élasticité et plasticité. *Journal de Mécanique Théorique et Appliquée* 1982; (spécial):45–59.

26. Qi W, Bertram A. Anisotropic continuum damage modelling for F.C.C.-single crystals at high temperatures. *International Journal of Plasticity* 1999; **15**(11):1197–1215.
27. Kachanov LM. Time of the rupture process under creep conditions. *Izvestiya Akademii Nauk SSSR Otdelenie Tekhnicheskikh* 1958; **8**:26–31.
28. Rabotnov YN. Creep rupture. *Proceedings of the 12th International Congress on Theoretical and Applied Mechanics* (ICTAM). Springer: Stanford, CA, U.S.A., 1969; 342–349.
29. Pellet F, Boidy E, Bouvard A, Hoteit N. Viscoplastic behavior and damage to rock related to the design of underground waste depository. *Proceedings of the 10th International Congress on Rock Mechanics*, Sandton, South-Africa, 2003; 893–898.
30. Shao JF, Hoxha D, Bart M, Homand F, Duveau G, Souley M, Hoteit N. Modelling of induced anisotropic damage in granites. *International Journal of Rock Mechanics and Mining Sciences* 1999; **36**:1001–1012.

